FITEE

Longitudinal and lateral slip control of autonomous wheeled mobile robot for trajectory tracking[*]

Hamza KHAN[1,2], Jamshed IQBAL[†‡3], Khelifa BAIZID[4], Teresa ZIELINSKA[1]

([1]*Division of Theory of Machines and Robots, Warsaw University of Technology, Warsaw 00-661, Poland*)

([2]*Department of Advanced Robotics, Istituto Italiano di Tecnologia, Genova 16163, Italy*)

([3]*Department of Electrical Engineering, COMSATS Institute of Information Technology, Islamabad 44000, Pakistan*)

([4]*Department of Electrical and Information Engineering, University of Cassino and Southern Lazio, Cassino 03043, Italy*)

[†]E-mail: jamshed.iqbal@comsats.edu.pk

Abstract: This research formulates a path-following control problem subjected to wheel slippage and skid and solves it using a logic-based control scheme for a wheeled mobile robot (WMR). The novelty of the proposed scheme lies in its methodology that considers both longitudinal and lateral slip components. Based on the derived slip model, the controller for longitudinal motion slip has been synthesized. Various control parameters have been studied to investigate their effects on the performance of the controller resulting in selection of their optimum values. The designed controller for lateral slip or skid is based on the proposed side friction model and skid check condition. Considering a car-like WMR, simulation results demonstrate the effectiveness of the proposed control scheme. The robot successfully followed the desired circular trajectory in the presence of wheel slippage and skid. This research finds its potential in various applications involving WMR navigation and control.

Key words: Robot modeling, Robot navigation, Slip and skid control, Wheeled mobile robots
doi:10.1631/FITEE.1400183   **Document code:** A   **CLC number:** TP24

1 Introduction

Innovations in mechatronic systems and allied research domains have witnessed an increasing trend in robot applications. These robots can be articulated (Iqbal *et al.*, 2012; Manzoor *et al.*, 2014) or mobile (Iqbal *et al.*, 2013). Most of the applications require robots to be mobile (Zohaib *et al.*, 2014a), thus bringing challenging issues regarding their interaction with the operating environment. These issues, in addition to slip/skid control, include navigation (Zohaib *et al.*, 2014b), localization (Krejsa and Vechet, 2012), obstacle avoidance (Adrian and Ribickis,

2013), and path planning (Ishigami *et al.*, 2007). The locomotion system of a mobile robot can be based on legs, tracks, or wheels.

Wheels exhibit efficient locomotion strategies. Keeping in viewing their inherent advantages, wheels become the most appropriate locomotion approach for most of the autonomous mobile robots. For a wheeled mobile robot (WMR), mobility and traversability are two main dynamics to accomplish a task. Wheel slip or skid directly affects both dynamics. Numerous controllers reported in the literature for autonomous WMRs have been developed considering the robot as a mechanical system with nonholonomic constraints, i.e., with non-slipping and non-skidding assumptions. Such assumptions may be justified, when a WMR moves with relatively low velocities and accelerations on a firm and adhesive track. There are many examples of conditions, such as motion on a slippery ground or low traction terrain, where

non-slipping and non-skidding assumptions are violated. So, for high-speed WMRs, such assumptions become unrealistic in terms of stability and control performance. Practically, wheel skidding and slipping are unavoidable especially with tire deformation and changes in track surface conditions.

Many solutions have been proposed to control wheel slippage of WMRs. A lot of work has already been done in the automobile industry regarding slip control. Traction control system (TCS) or anti-slip regulation (ASR) is used for slip control in modern vehicles. Such control systems are specifically designed to avoid loss of traction and to enhance driver control. Consequently, they help to reduce the mismatch between applied and required torques, where applied torque depends on throttle input and required torque depends on road surface conditions and other varying factors. Normally, TCS or ASR shares the electro-hydraulic brake actuator and wheel speed sensors with the anti-lock braking system. These controls take throttle or spark sequence as the main input to control the applied torque. Using the same idea of TCS or ASR, many authors proposed traction control for electronic vehicles or WMRs. Pusca *et al.* (2002) proposed a traction control algorithm for a four-wheeled electric vehicle. This algorithm, being widely used for WMRs, aims to handle and stabilize the robot during slip or skid. The drawback of this algorithm is its specific application to the family of WMRs in which each wheel is driven by a separate drive, which leads to more power consumption. Sidek and Sarkar (2008) proposed a nonlinear feedback controller to develop the relationship between the dynamic torque given to the motor and the available traction force. In this model, the dynamic torque taken in slip dynamics uses a Lagrangian approach and generates traction force as a function of wheel slip. The accuracy of these approaches depends upon the model of slip ratio or slip angle. Li *et al.* (2006) modeled wheel-ground interaction and derived conditions for robots to avoid slip for both torque and motion. However, this approach does not detect actual slip of the wheels and therefore traction control on WMRs has not been implemented.

Different models have been proposed for frictional coefficient in case of longitudinal and lateral slip. These models depend mainly on the type of terrain, road-wheel interaction, and speed of WMRs. For longitudinal slip control, the coefficient of friction as a function of slip ratio was modeled in Zielinska and Chmielniak (2010). With this model one can theoretically estimate longitudinal slip of WMRs. However, it does not consider lateral slip. Considering outdoor applications of WMRs, Sánchez-Hermosilla *et al.* (2010) presented an autonomous robot for agriculture. Assuming low velocity of the robot, only longitudinal slip has been taken into account. Ding *et al.* (2010) presented a highly precise terramechanics model to predict longitudinal slip-sinkage. It has been found that wheel lugs have a slight influence on sinkage. Using a custom-developed wheel-soil interaction testbed, experimental results were reported in Ding *et al.* (2011) to study the influence of various parameters like wheel's radius and width, vertical load, resistance coefficients, etc. on driving performance. These studies were focused on longitudinal slip. Similarly, model-based slippage detection algorithms reported in Ward and Iagnemma (2008) and Ani *et al.* (2013) neglect lateral skid forces. For skid prediction, Gao *et al.* (2013) presented an improved empirical model for space rovers based on a model of terrestrial vehicles conceived by Wong and Reece (1967). Using an iterative optimization approach, a variant sinkage exponent is iteratively changed for skid prediction. Recently, Ding *et al.* (2013) have compared slip and skid mechanics by proposing a piece-wise linear function to predict the resistance moment and the drawbar pull in both conditions. They also predicted skid mechanics based on the slip mechanics using a semi-empirical formulation.

The detailed literature review revealed that there are a number of reported studies pertaining to the traction of WMRs. Most of these were limited to the consideration of the longitudinal characteristics of a robot's wheel. Only a few studies deeply investigated the lateral skid. Wheel-terrain interaction principles for slip and skid are quite different, while the latter is crucial in steering maneuver analysis of a robot. The primary contribution of the present research lies in consideration of wheel slippage as well as its skidding in case of a car-like WMR. The derived model and results obtained can find potential in analysis of the wheel-ground interaction process and optimization of wheel design.

2 Longitudinal motion slip control

The desired trajectory is a straight line to encounter longitudinal wheel slip. This trajectory is enough to model the driven wheel as the simulation implies, without involving steering action. Table 1 shows the nomenclature of the control law for longitudinal slip derived in Zielinska and Chmielniak (2010).

Table 1 Nomenclature

Symbol	Description
m	Part of the robot mass supported by the wheel
Q	Force acting on the wheel shaft
r	Radius of the wheel
f_0	Rolling resistance coefficient
μ_0	Wheel-ground cohesion coefficient
p	Normalized radius of the wheel-ground contact
M_e	Torque due to the additional external factors
μ_c	Virtual friction coefficient
$\lambda(t)$	Slip ratio (a function of time)
e	Error signal (difference between reference and real values)
λ_M	Slip obtained by using the slip decrease model
λ_R	Real slip
k_p, k_v	Controller gains

The condition for wheel angular velocity ($\ddot{\phi}$) not causing slip is written as

$$\ddot{\phi} \leq \frac{\mu_c Qr - f_0 Qr - \mu_0 Qp - M_e}{J + mr^2},\qquad(1)$$

where μ_c is a function of $\lambda(t)$ and J is the inertia momentum of the robot. The proposed conservative model for the critical slip coefficient exponentially depends on $\lambda(t)$. The model of critical slip coefficient can be written as

$$J\ddot{\phi} + mr^2[\ddot{\phi}(1 - \lambda(t)) - \dot{\phi}\dot{\lambda}(t)]$$
$$= \mu_c \exp\left(-\frac{\lambda^2(t)}{b}\right)Qr,\qquad(2)$$

where b is a constant defining friction as a function of slip distance. $b=0.26$ for $\mu_c \leq 0.9$ is a good approximation as discussed in Zielinska and Chmielniak (2010).

For Eq. (2), the control signal (T_C) is

$$T_C = [J + mr^2(1 - \lambda_M)](\ddot{\phi} + k_v\dot{e} + k_p e) - \dot{\phi}\dot{\lambda}_M mr^2.\quad(3)$$

Corresponding to the real position (ϕ), the real torque (T_R) is given by

$$T_R = [J + mr^2(1 - \lambda_R)]\ddot{\phi} - \dot{\phi}\dot{\lambda}_R mr^2.\qquad(4)$$

For stability, the difference between produced and real torques ($T_R - T_C$) must be zero ($T_R = T_C$). Based on this condition, the control law for longitudinal slip is given by Eq. (5) and illustrated in Fig. 1.

$$\ddot{e} + k_v\dot{e} - \frac{mr^2\dot{\lambda}_M}{1 + mr^2(1 - \lambda_M)}\dot{e} + \frac{k_p}{1 + mr^2(1 - \lambda_M)}e$$
$$= \frac{1}{1 + mr^2(1 - \lambda_M)}[(\lambda_M - \lambda_R)\ddot{\phi} + mr^2(\dot{\lambda}_M - \dot{\lambda}_R)\dot{\phi}].\quad(5)$$

3 Lateral motion slip control

Lateral slip or skid results in kinematic perturbations, which include slip angle and lateral velocity. The main goal of the designed controller is to cancel or minimize the effect of these perturbations and keep a WMR on a desired circular path. For the present research, the Dugoff model (Dakhlallah *et al.*, 2008) is selected owing to two main reasons: the model needs a smaller number of parameters to evaluate the tire/road forces, and the formulation remains close to the linear formulation. Consider a four-wheeled robot with two front steering wheels and two rear fixed wheels (Fig. 2). The dynamic model of the robot representing the longitudinal and lateral translational motions and the yaw rotational movement is given by

$$m\dot{V}_X = \sum_{i=1}^{4} F_{Xi} + m\dot{\theta}V_Y,\qquad(6)$$

$$m\dot{V}_Y = \sum_{i=1}^{4} F_{Yi} + m\dot{\theta}V_X,\qquad(7)$$

$$I_Z\ddot{\theta} = \sum_{i=1}^{4} M_{Zi},\qquad(8)$$

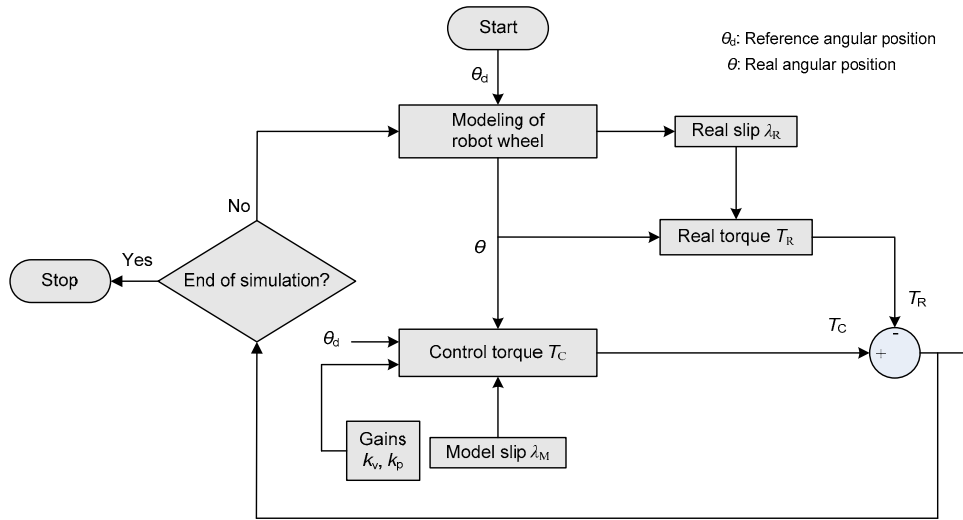where V_X and V_Y are longitudinal and lateral velocities
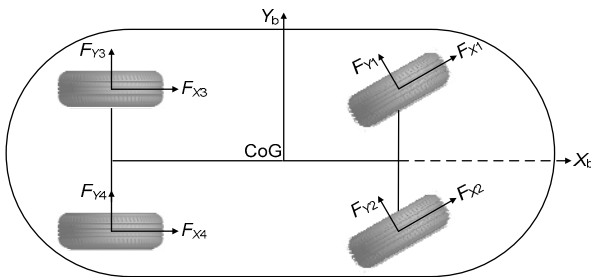
Fig. 1 Block diagram of the slip control law

Fig. 2 Robot and external forces (CoG: center of gravity)

of the vehicle, respectively, θ is the yaw angle, I_Z is the moment of inertia around the vertical axis, F_{Xi} and F_{Yi} are the longitudinal and lateral tire/road forces respectively, M_{Zi} is the vertical rotational moment, and subscript i (i=1, 2, 3, 4) indicates the specific wheel of the vehicle.

The scientific analysis of skid demands a friction model in a circular horizontal curve. Supply of friction depends on the robot velocity and interaction of wheels with the operating surface. In the automobile industry, a well-known mathematical model, the Pennsylvania model (Kulakowski, 1991), has been reported for lateral friction:

$$F(S) = F_0 \mathrm{e}^{-S/S_0}, \tag{9}$$

where $F(S)$ is the friction coefficient at velocity S of the wheel in contact with the road, F_0 is the static skid number, empirically related with texture and skid resistance, and S_0 is a constant value that has unit of

velocity (km/h) and depends mainly on the texture of pavement. The Pennsylvania model is used for high-speed vehicles whereas the speed and mass of a WMR are comparably low. So, we propose a model given by Eq. (10) for side friction supply, which depends on tire-surface interaction and WMR speed:

$$u(v) = \mu_s \mathrm{e}^{-V/V_0}, \tag{10}$$

where μ_s is the friction coefficient between the surface of the track and the tyres of WMR. In this case, a WMR is considered as a point mass, and thus V is the velocity (m/s) of the point mass moving along the curve and V_0 is a constant with unit of m/s. The lateral friction on the tires of WMR is proportional to the mass and type of terrain. Normally, a coefficient of friction is given for the two materials involved to describe the behavior of the terrain. Using the lateral friction mathematical model (10), the sum of frictional (F_{ff}) or lateral forces acting on WMRs while moving on circular path can be written as

$$F_{\mathrm{ff}} = \mu_s \mathrm{e}^{-V/V_0} \sum_{i=1}^{4} F_{Yi}, \tag{11}$$

where $\sum_{i=1}^{4} F_{Yi}$ is the sum of lateral forces acting on wheels of the WMR from Eq. (7). When a WMR takes a turn, external forces act on the front and rear wheels. The force required by a WMR to hold on the

horizontal curve while in motion, i.e., curve resistance (R_c), depends on the radius of the horizontal curve and the speed of the robot. It can be defined as

$$R_c = \frac{V^2}{R}m, \tag{12}$$

where R is the radius of curvature. Using Eqs. (11) and (12), the skid condition can then be written as

$$\mu_s e^{-V/V_0} \sum_{i=1}^{4} F_{Yi} \le \frac{V^2}{R}m. \tag{13}$$

Eq. (13) states that as a WMR moves along a circular horizontal curve, if the sum of all lateral forces acting on the robot is not larger than the curve resistance, the WMR undergoes skid mode or would tend to run off the curve following a tangential path. As the WMR moves on a horizontal curve, the supply of side friction decreases with the increase in speed and thus reduces the grip of lateral forces acting on wheel-ground contact points of the WMR. From Eq. (13), it is clear that we can reduce the demand curve resistance by reducing the velocity of a WMR and by increasing the radius of the circular horizontal curve. Based on Eq. (13), once a skid is encountered, the task of the designed controller is to generate a controlled steering angle to make the robot follow the desired trajectory by mitigating the skidding effect.

4 Results and discussion

To test the proposed strategy, the slip controller was subjected to an input signal written in the Laplace domain as

$$\phi(s) = A \frac{\omega_n^2}{s(s^2 + 2\eta\omega_n s + \omega_n^2)}, \tag{14}$$

where A is the reference value for the wheel position, ω_n is the natural frequency, and η is the damping ratio. Real and reference input signals are shown in Fig. 3 with a reference having a unity delay for the simulation.

Various parameters with different values, including natural frequency, damping ratio, mass, and radius, have been adjusted to find a faster and smoother response. To select a suitable natural frequency, its different values have been tested against different values of other parameters. The observations indicate that increasing the frequency of the input control signal, oscillations in controller response also start increasing. Fig. 4a shows the controller responses under different natural frequencies when the mass is fixed to 1 kg and radius of wheel fixed to 0.03 m. Responses corresponding to a mass of 5 kg and a radius of 0.1 m are illustrated in Fig. 4b. It is observed that the responses under the same natural frequency but different masses and radii are very similar. This implies that changes in radius and mass do not affect the responses. In both cases, the response quickly converges to a steady state when ω_n is between 0.5 and 1.0.
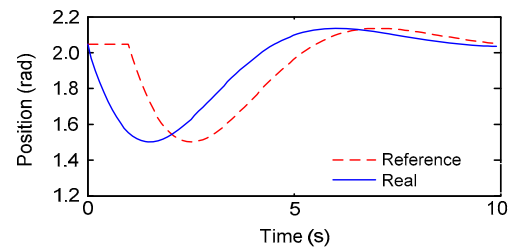
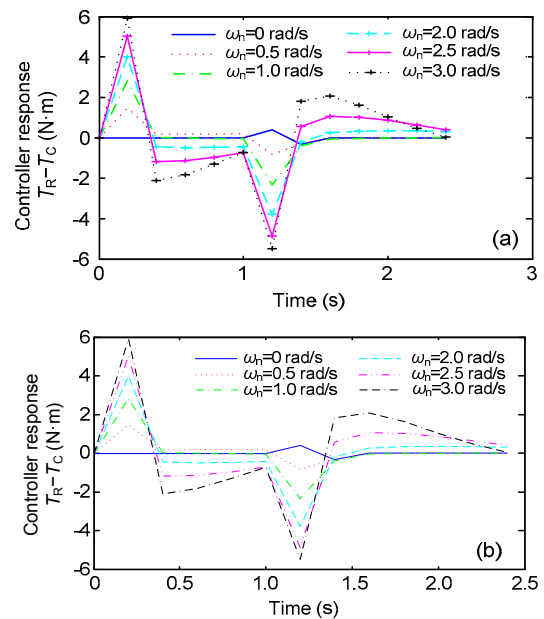

Fig. 3 Reference and real angular positions of wheel

Fig. 4 Controller responses under various natural frequencies
(a) m=1 kg, r=0.03 m; (b) m=5 kg, r=0.1 m

Increasing the damping ratio (η) of the input signal, the oscillations increase. When $\eta=0.5$, the response is precise and converges to a steady state most quickly (Fig. 5a). In another test, when the mass supported by the wheel has been increased from 0.9 to 25 kg while keeping $r=0.02$ m, the controller responses show an increase in overshoot (Fig. 5b).

Finally, the radius of a wheel with a fixed supported mass of 0.9 kg has been varied from 0.02 to 0.40 m. Results indicate a rapid increase in overshoot (Fig. 6).

The overall results indicate that when increasing the mass supported by the wheel, we need to increase the radius of the wheel for a suitable controller response. Otherwise, with an increase in mass and a decrease of wheel radius or vice versa, unsuitable controller responses would cause wheel slipping. Table 2 shows the optimum natural frequencies and damping ratios at different values of mass supported by the wheel and its radius.

Simulation has been carried out in MATLAB/ Simulink to show how a WMR can negotiate skidding while moving along a circular path. Fig. 7a shows poorly tuned results. The deviations from the reference path are obvious. A better tuning of the controller resulted in a trajectory which well matches the reference trajectory (Fig. 7b).

Table 2 Optimum selection of natural frequencies and damping ratios

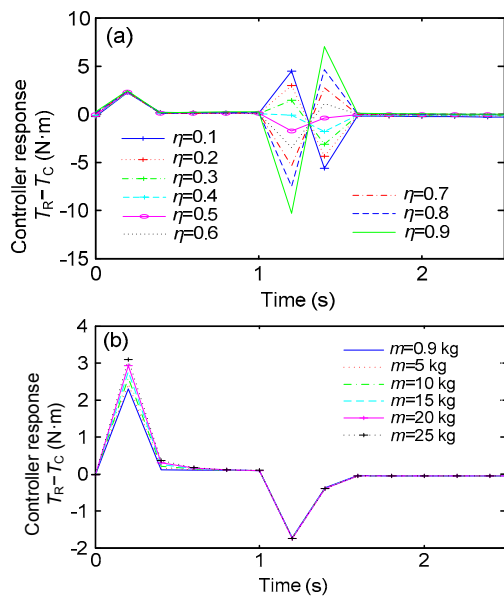| m/r (kg/m)	ω_n (rad/s)	η	m/r (kg/m)	ω_n (rad/s)	η
0.5/0.01	0.67	0.41	5.0/0.06	0.75	0.59
0.9/0.02	0.73	0.53	7.0/0.10	0.66	0.76
1.0/0.03	0.69	0.51			

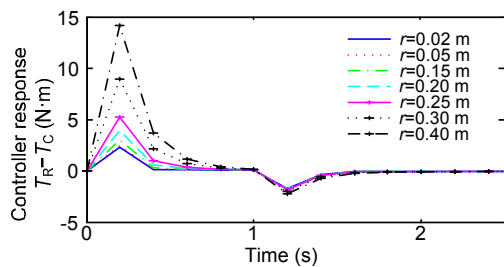**Fig. 5 Controller responses under various damping ratios (a) and masses (b)**

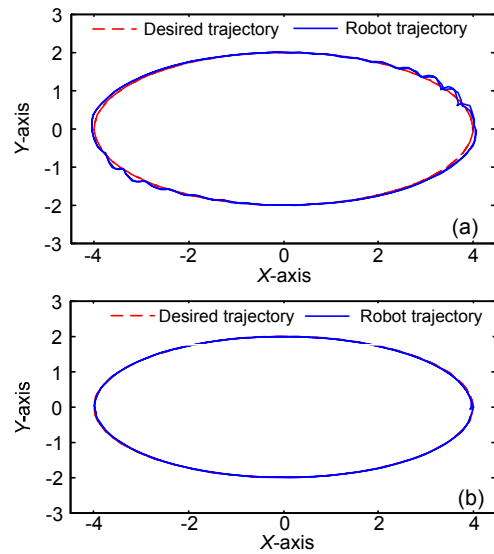**Fig. 6 Controller responses under various radii**

Fig. 7 Trajectories followed by the robot with the proposed controller under poorly tuned case (a) and well tuned case (b)

5 Conclusions

A novel scheme to mitigate the effects of WMRs' wheel slippage and skidding using the designed controllers has been proposed and tested. The objective of the skid controller is to minimize the effects of kinematic perturbations and thus to keep the robot on a desired circular trajectory. Tests have been conducted to select suitable parameters for the

controller to achieve faster and smoother response. Different parameters have been studied and investigated closely to examine their effects on each other. We have achieved uniform boundedness with exponentially converging errors without imposing restrictive assumptions on the skidding and slipping perturbations. To further characterize robustness of the controller and analyze its performance more critically, the proposed control scheme is currently being implemented on the custom-developed research platform (Ahmad *et al.*, 2014).

References

Adrian, L.R., Ribickis, L., 2013. Fuzzy logic analysis of photovoltaic data for obstacle avoidance or mapping robot. *Elektron. Elektrotech.*, **19**(1):3-6. [doi:10.5755/j01.eee.19.1.3243]

Ahmad, O., Ullah, I., Iqbal, J., 2014. A multi-robot educational and research framework. *Int. J. Acad. Res.*, **6**(2):217-222.

Ani, O.A., Xu, H., Shen, Y.P., *et al.*, 2013. Modeling and multiobjective optimization of traction performance for autonomous wheeled mobile robot in rough terrain. *J. Zhejiang Univ.-Sci. C (Comput. & Electron.)*, **14**(1):11-29. [doi:10.1631/jzus.C12a0200]

Dakhlallah, J., Glaser, S., Mammar, S., 2008. Tire-road forces estimation using extended Kalman filter and sideslip angle evaluation. American Control Conf., p.4597-4602. [doi:10.1109/ACC.2008.4587220]

Ding, L., Gao, H., Deng, Z., *et al.*, 2010. Wheel slip-sinkage and its prediction model of lunar rover. *J. Cent. South Univ. Technol.*, **17**(1):129-135. [doi:10.1007/s11771-010-0021-7]

Ding, L., Gao, H., Deng, Z., *et al.*, 2011. Experimental study and analysis on driving wheels' performance for planetary exploration rovers moving in deformable soil. *J. Terramech.*, **48**(1):27-45. [doi:10.1016/j.jterra.2010.08.001]

Ding, L., Gao, H., Deng, Z., *et al.*, 2013. Longitudinal slip versus skid of planetary rovers' wheels traversing on deformable slopes. Proc. IEEE/RSJ Int. Conf. on Intelligent Robots and Systems, p.2842-2848. [doi:10.1109/IROS.2013.6696758]

Gao, H., Guo, J., Ding, L., *et al.*, 2013. Longitudinal skid model for wheels of planetary exploration rovers based on terramechanics. *J. Terramech.*, **50**(5-6):327-343. [doi:10.1016/j.jterra.2013.10.001]

Iqbal, J., Islam, R.U., Khan, H., 2012. Modeling and analysis of a 6 DOF robotic arm manipulator. *Can. J. Electr. Electron. Eng.*, **3**(6):300-306.

Iqbal, J., un Nabi, S.R., Khan, A., *et al.*, 2013. A novel track-drive mobile robotic framework for conducting projects on robotics and control systems. *Life Sci. J.*, **10**(3):130-137.

Ishigami, G., Miwa, A., Nagatani, K., *et al.*, 2007. Terramechanics-based model for steering maneuver of planetary exploration rovers on loose soil. *J. Field Robot.*, **24**(3):233-250. [doi:10.1002/rob.20187]

Krejsa, J., Vechet, S., 2012. Infrared beacons based localization of mobile robot. *Elektron. Elektrotech.*, **117**(1):17-22. [doi:10.5755/j01.eee.117.1.1046]

Kulakowski, B.T., 1991. Mathematical model of skid resistance as a function of speed. *In*: Pavement Management: Data Collection, Analysis, and Storage. Transportation Research Board, USA, p.26-33.

Li, Y.P., Zielinska, T., Ang, V.M.H., *et al.*, 2006. Wheel-ground interaction modelling and torque distribution for a redundant mobile robot. Proc. IEEE Int. Conf. on Robotics and Automation, p.3362-3367. [doi:10.1109/ROBOT.2006.1642215]

Manzoor, S., Islam, R.U., Khalid, A., *et al.*, 2014. An open-source multi-DOF articulated robotic educational platform for autonomous object manipulation. *Robot. Comput.-Integr. Manuf.*, **30**(3):351-362. [doi:10.1016/j.rcim.2013.11.003]

Pusca, R., Ait-Amirat, Y., Berthon, A., *et al.*, 2002. Modeling and simulation of a traction control algorithm for an electric vehicle with four separate wheel drives. Proc. IEEE 56th Vehicular Technology Conf., p.1671-1675. [doi:10.1109/VETECF.2002.1040500]

Sánchez-Hermosilla, J., Rodríguez, F., González, R., *et al.*, 2010. A mechatronic description of an autonomous mobile robot for agricultural tasks in greenhouses. *In*: Barrera, A. (Ed.), Mobile Robots Navigation. InTech, Croatia, p.583-607.

Sidek, N., Sarkar, N., 2008. Dynamic modeling and control of nonholonomic mobile robot with lateral slip. Proc. 3rd Int. Conf. on Systems, p.35-40. [doi:10.1109/ICONS.2008.22]

Ward, C.C., Iagnemma, K., 2008. A dynamic-model-based wheel slip detector for mobile robots on outdoor terrain. *IEEE Trans. Robot.*, **24**(4):821-831. [doi:10.1109/TRO.2008.924945]

Wong, J.Y., Reece, A.R., 1967. Prediction of rigid wheel performance based on the analysis of soil-wheel stresses: Part II. Performance of towed rigid wheels. *J. Terramech.*, **4**(2):7-25. [doi:10.1016/0022-4898(67)90047-X]

Zielinska, T., Chmielniak, A., 2010. Controlling the slip in mobile robots. Proc. 13th Int. Conf. on Climbing and Walking Robots and the Support Technologies for Mobile Machines, p.13-20.

Zohaib, M., Pasha, S.M., Javaid, N., *et al.*, 2014a. An improved algorithm for collision avoidance in environments having U and H shaped obstacles. *Stud. Inform. Contr.*, **23**(1):97-106.

Zohaib, M., Pasha, S.M., Javaid, N., *et al.*, 2014b. IBA: intelligent bug algorithm—a novel strategy to navigate mobile robots autonomously. Proc. 3rd Int. Multi-topic Conf., p.291-299. [doi:10.1007/978-3-319-10987-9_27]